MPMI Vol. 25, No. 9, 2012, pp. 1238–1250. http://dx.doi.org/10.1094/MPMI-02-12-0033-R. © 2012 The American Phytopathological Society *e*-Xtra*

Recognition of Avirulence Gene *AvrLm1* from Hemibiotrophic Ascomycete *Leptosphaeria maculans* Triggers Salicylic Acid and Ethylene Signaling in *Brassica napus*

Vladimír Šašek,[1,2] Miroslava Nováková,[1,3] Barbora Jindřichová,[1] Károly Bóka,[4] Olga Valentová,[3] and Lenka Burketová[1]

[1]Institute of Experimental Botany, Academy of Sciences of the Czech Republic, Na Karlovce 1a, 160 00 Prague 6, Czech Republic; [2]Department of Plant Protection, Czech University of Life Sciences Prague, Kamýcká 129, 165 21 Prague 6, Czech Republic; [3]Department of Biochemistry and Microbiology, Institute of Chemical Technology Prague, Technická 5, 166 28 Prague 6, Czech Republic; [4]Department of Plant Anatomy, Eötvös Loránd University, Pázmány Péter sétány 1/C, H-1117, Hungary

Submitted 12 February 2012. Accepted 13 May 2012.

Interaction of a plant with a fungal pathogen is an encounter with hundreds of molecules. In contrast to this, a single molecule often decides between the disease and resistance. In the present article, we describe the defense responses triggered by *AvrLm1,* an avirulence gene from a hemibiotrophic ascomycete, *Leptosphaeria maculans*, responsible for an incompatible interaction with *Brassica napus*. Using multiple hormone quantification and expression analysis of defense-related genes, we investigated signaling events in *Rlm1* plants infected with two sister isolates of *L. maculans* differentiated by the presence or absence of *AvrLm1*. Infection with the isolate carrying *AvrLm1* increased the biosynthesis of salicylic acid (SA) and induced expression of the SA-associated genes *ICS1*, *WRKY70*, and *PR-1,* a feature characteristic of responses to biotrophic pathogens and resistance gene–mediated resistance. In addition to SA-signaling elements, we also observed the induction of *ASC2a, HEL*, and *CHI* genes associated with ethylene (ET) signaling. Pharmacological experiments confirmed the positive roles of SA and ET in mediating resistance to *L. maculans.* The unusual cooperation of SA and ET signaling might be a response to the hemibiotrophic nature of *L. maculans*. Our results also demonstrate the profound difference between the natural host *B. napus* and the model plant *Arabidopsis* in their response to *L. maculans* infection.

Fungi use different strategies to colonize plants. Necrotrophs kill the host cells during infection and derive nutrients from the dead tissue. In contrast, biotrophs parasitize living cells over a long period. For some species, termed hemibiotrophs, the initial period of infection is biotrophic, followed by a destructive necrotrophic phase (Perfect and Green 2001). Plants sense pathogens by a battery of transmembrane receptors (Dodds and Rathjen 2010). The signals triggered after recognition of the pathogen-associated molecules are transmitted through a complex network controlled by plant hormones. In the model plant *Arabidopsis thaliana*, defenses against biotrophic pathogens are regulated mainly by salicylic acid (SA) signaling, whereas jasmonic acid (JA) together with ethylene (ET) regulate responses to necrotrophs (Oliver and Ipcho 2004). Other hormones, such as abscissic acid, auxin, gibberellins, and cytokinins, have also been shown to modulate plant defenses, albeit to a lesser extent. Specific activation of signaling pathways allows the plant to fine-tune its defense responses (Pieterse et al. 2009).

Genomes of fungal pathogens encode hundreds of secreted effectors promoting virulence (Schmidt and Panstruga 2011). Many of these effectors interfere with plant signaling pathways so as to prevent activation of defense mechanisms. The ability to overcome plant basal resistance by means of effectors differentiates pathogens from nonpathogens. During the coevolution with biotrophs and hemibiotrophs, plants acquired another layer of defense mechanisms by which cytosolic receptors directly or indirectly recognize some effectors. These receptors were shown to be encoded by many previously known resistance (*R*) genes from various plant species (Jones and Dangl 2006). A recognized effector is termed an avirulence (Avr) protein. A plant carrying an *R* gene that is resistant to a pathogen with the corresponding *Avr* gene results in an incompatible interaction. The pathogen can become virulent when it alters or completely eliminates the *Avr* gene. This frequently occurs in the field due to high selection pressure caused by massive cultivation of crops with a single *R* gene (McDonald and Linde 2002). Incompatible interaction is associated with massive production of reactive oxygen species (ROS). ROS directly damage the pathogen, strengthen the plant cell walls, and mediate a hypersensitive response (HR) (Torres et al. 2006). An HR can be characterized by cytological and physiological alterations and the rapid death of cells localized around the infection site (Mittler and Lam 1995). Although HR is a hallmark of incompatible interaction, it is not always required to restrict pathogen growth (Yu et al. 1998). Although SA has been shown to play a major role in *R* gene–mediated resistance, ET and JA signaling pathways also seem to contribute, albeit to a lesser extent and redundantly (Tsuda et al. 2009). In contrast to biotrophic fungi, resistance mediated by *R* genes was not found in interactions with necrotrophs.

Corresponding author: L. Burketová; E-mail: burketova@ueb.cas.cz

*The *e*-Xtra logo stands for "electronic extra" and indicates that one supplementary figure and one supplementary table are published online and that Figures 3 and 8 appear in color online.

Leptosphaeria maculans is a hemibiotrophic ascomycete and causal agent of phoma stem canker of oilseed rape (*Brassica napus*) causing serious losses in Europe, Australia, and North America (Fitt et al. 2006). Colonization of a plant begins with infection of cotyledons or the first true leaves by ascospores or, later in the season, by conidia. During the initial phase of infection, the fungus is biotrophic and colonizes the leaf mesophyll without causing any visible symptoms. After several days, the pathogen switches to a necrotrophic lifestyle and lesions with pycnidia appear on the leaves (Hammond and Lewis 1987). During the following period, *L. maculans* grows asymptomatically through petiole to the stem base, where it causes severe necrosis.

The most common and effective way to control *L. maculans* is to breed resistant cultivars. *R* genes have been identified in *B. napus* or have been introduced from related species (Delourme et al. 2006). The *R* gene–mediated resistance is manifested during the leaf infection and operates under the standard gene-for-gene concept. In some *B. napus* cultivars, another type of resistance was found effective against stem base necrosis. It is supposed to be encoded by multiple genes and is postulated to be race nonspecific (Delourme et al. 2006). At least 11 *R* genes have been identified in *Brassica* spp., with at least 9 corresponding *Avr* genes (*AvrLm1 to AvrLm9*) in *L. maculans.* Whereas no *R* gene has been cloned in *B. napus,* three *Avr* genes (*AvrLm1*, *AvrLm6*, and *AvrLm4-7)* already were identified (Fudal et al. 2007; Gout et al. 2006; Parlange et al. 2009). All three genes were annotated as small, secreted proteins with no or low similarity to proteins from other fungi and, therefore, are expected to act as effectors. Recently, the sequencing of the *L. maculans* genome uncovered hundreds of other putative effectors (Rouxel et al. 2011). *L. maculans* also secretes a major non-host-specific toxin, sirodesmin PL, and one toxin, phomalide, postulated to be host-selective (Rouxel and Balesdent 2005). Although the genetics of *B. napus* resistance has been intensively studied, very little is known about the function of the particular *R* genes and defense mechanisms involved. Resistance against *L. maculans* can be induced by the SA analogue benzothiadiazole (BTH) and the infection is associated with SA marker gene induction. Transformation of *B. napus* plants with the salicylate hydroxylase gene *nahG* has been shown to increase plant susceptibility to the pathogen (Potlakayala et al. 2007).

Much more work has been done on *Arabidopsis* to elucidate its mechanisms of resistance to *L. maculans*. *Arabidopsis* plants are non-host to *L. maculans* (Bohman et al. 2004) but the loss of a single Toll interleukin-1 receptor–nucleotide binding–leucine-rich repeat *R* gene allows the fungus to colonize the plant and form pycnidia. Resistance mediated by this gene seems to require callose deposition (Staal et al. 2006). Defense responses have been investigated further in plants lacking the *R* gene. Defense responses in these plants are mediated by JA. Introduction of a mutation in the key JA signaling regulator *coi1* has been shown to result in a hypersusceptible phenotype. Interestingly, when the ET signaling mutant *ein2* was co-introduced with *coi1*, the phenotype reverted back to moderate susceptibility (Persson et al. 2009). Oxidative burst and abscissic acid are also important for *Arabidopsis* resistance to *L. maculans* (Kaliff et al. 2007). Recently, Jindrichova and associates (2011) investigated the role of ROS during the compatible interaction of *L. maculans* with *B. napus*, showing that the fungus might benefit from ROS accumulation during the phase of lesion formation.

Current knowledge of resistance mechanisms against *L. maculans* is based mainly on studies performed on the model plant *Arabidopsis.* Therefore, it is necessary to investigate these mechanisms in the natural host. The aim of this work is to describe mechanisms of resistance triggered during the incompatible interaction of oilseed rape with *L. maculans* carrying the *Avr* gene *AvrLm1*. Defense responses, including hormone signaling, hydrogen peroxide formation, and callose deposition during infection with an avirulent isolate, were compared with responses to a virulent isolate lacking the *AvrLm1* gene.

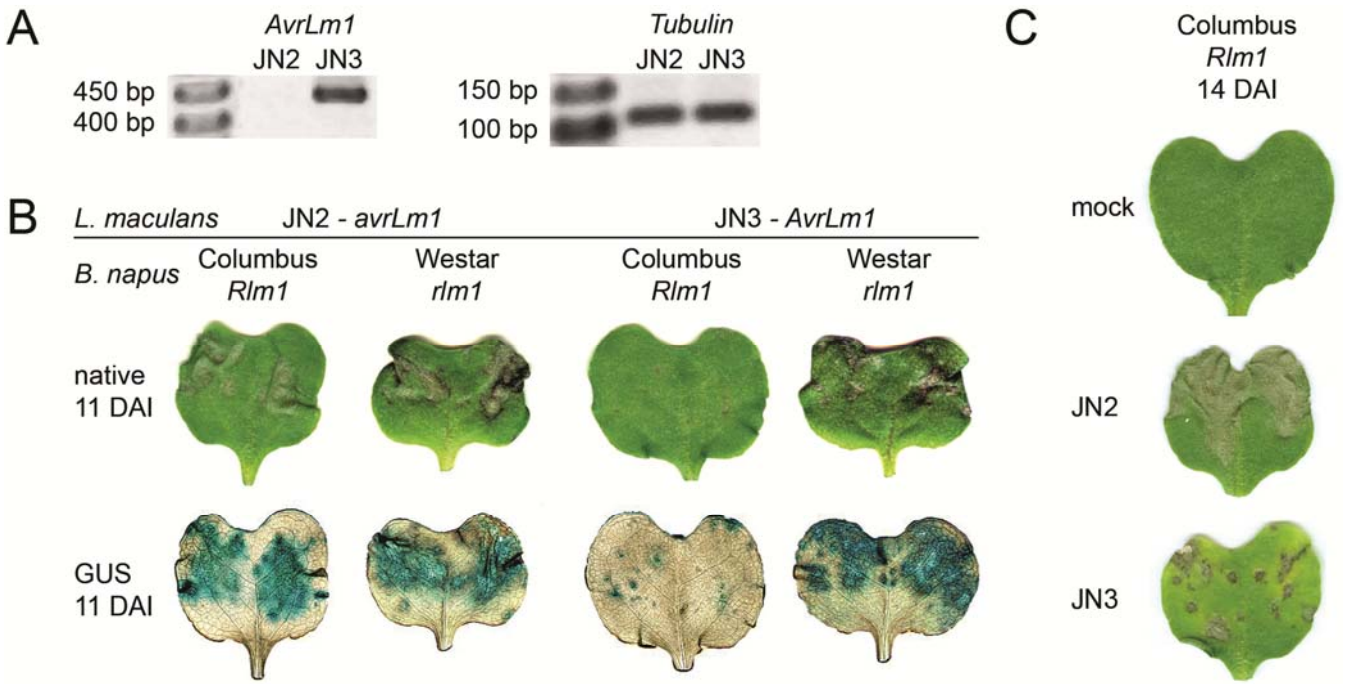

Fig. 1. Compatible and incompatible interactions of *Brassica napus* with *Leptosphaeria maculans.* **A,** Polymerase chain reaction (PCR) detection of gene *AvrLm1* in *L. maculans* isolates JN2 and JN3. *Tubulin* was used as a control for equal loading of DNA into the PCR reaction. **B,** Disease symptoms and mycelia stained by β-glucuronidase (GUS) activity in *B. napus* cotyledons 11 days after inoculation (DAI) with *L. maculans* spore suspension (10^5/ml). JN3 (*AvrLm1*) is avirulent on *B. napus* 'Columbus' carrying resistance gene *Rlm1* but causes normal symptoms in 'Westar' lacking the resistance gene. JN2 (*avrLm1*) is virulent on both *B. napus* cultivars. **C,** Disease symptoms on *B. napus* Columbus cotyledons 14 DAI with *L. maculans* isolates JN2 and JN3.

RESULTS

Incompatible interaction of *L. maculans* with *B. napus* determined by *AvrLm1*.

To study defense responses specifically triggered during incompatible interaction, we took two *L. maculans* isolates originating from one in vitro cross differing in the allele of *Avr* gene *AvrLm1* (Balesdent et al. 2001). We analyzed their interaction with plants of *B. napus* 'Columbus' carrying the corresponding *R* gene, *Rlm1*. Both isolates were transformed with bacterial β-glucuronidase (GUS) that enabled us to visualize the fungal mycelium in the infected tissue and investigate the relationship between the lesion size and mycelial growth (Fig. 1B). The difference in virulence between the isolates was shown to be mediated solely by *AvrLm1* because complementation of the virulent isolate JN2 with the *AvrLm1* genomic sequence of the avirulent isolate JN3 resulted in an incompatible interaction with all 16 tested *Rlm1* cultivars (Gout et al. 2006). We confirmed the correct attribution of *AvrLm1* by polymerase chain reaction (PCR) with primers designed for the published sequence (Fig. 1A). Resistance of *B. napus* cultivars to *L. maculans* is traditionally determined by puncture inoculation. This method, however, is not favorable for investigation of defense response because relatively few cells around the puncture are affected by the infection.

Therefore, we infiltrated the spore suspension into the intercellular space of the entire cotyledon, so that a number of plant cells could respond to the same stage of infection. Using the infiltration method, the differences in compatibility on *Rlm1* plants were clearly visible as a traditional puncture inoculation. Isolate JN2 caused large necrotic lesions 11 days after inoculation (DAI) on *B. napus* Columbus carrying the *R* gene *Rlm1,* whereas isolate JN3 caused weak symptoms resembling macroscopic HR (Fig. 1B). Small, dark-brown lesions were deeply embedded in the cotyledon tissue. However, the small lesions caused by JN3 were not restricted and spread further. At 14 DAI, JN3-infected cotyledons showed small, grayish lesions with sharp margins surrounded by weak chlorosis (Fig. 1C). A necrotic lesion caused by both isolates was associated with the mycelium at 11 DAI (Fig. 1B). Whereas mycelium of JN3 remained restricted to small spots around the lesions, the hyphal front of JN2 grew beyond the lesion to colonize the healthy tissue. Moreover, at that time, we could see clearly the formation of pycnidia in the compatible interaction of JN2 with *Rlm1* plants. We wanted to confirm that the difference in virulence between JN2 and JN3 on *B. napus* Columbus is a result of *AvrLm1* recognition and not of another genetic varia-

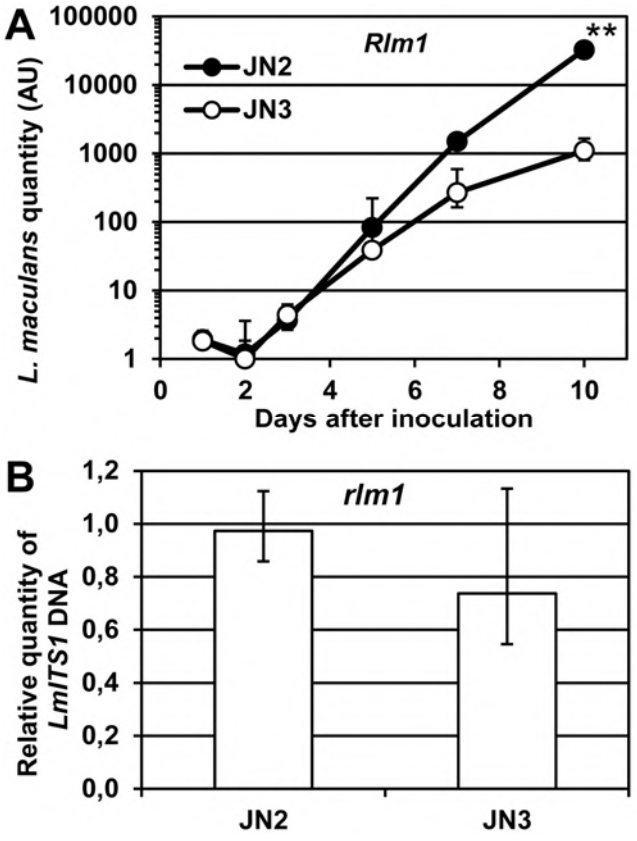

Fig. 2. A, Growth of *Leptosphaeria maculans* isolates JN2 and JN3 in infected tissue of *Brassica napus* 'Columbus' carrying gene *Rlm1*. Fungal mass was determined in cotyledons by reverse-transcription quantitative polymerase chain reaction (qPCR) of constitutively expressed *LmITS1*. Plants (11 days old) were inoculated by infiltration of spore suspension (10^5/ml). Expression of *LmITS1* was normalized to expression of *B. napus Actin.* Values represent means ± standard error (SE) from three independent experiments. Asterisks indicate statistically significant differences between isolates ($P < 0.05$, Student's *t* test). **B,** Quantity of *L. maculans* isolates JN2 and JN3 in cotyledons of susceptible (*rlm1*) 'Westar' 7 days after inoculation determined by qPCR quantification of *LmITS1* DNA. Data were normalized to the DNA quantity of plant *Actin*. Plants (11 days old) were inoculated by infiltration of spore suspension (10^5/ml). Values represent means ± SE from three biological replicates. Differences between isolates were statistically insignificant ($P < 0.05$; Student's *t* test).

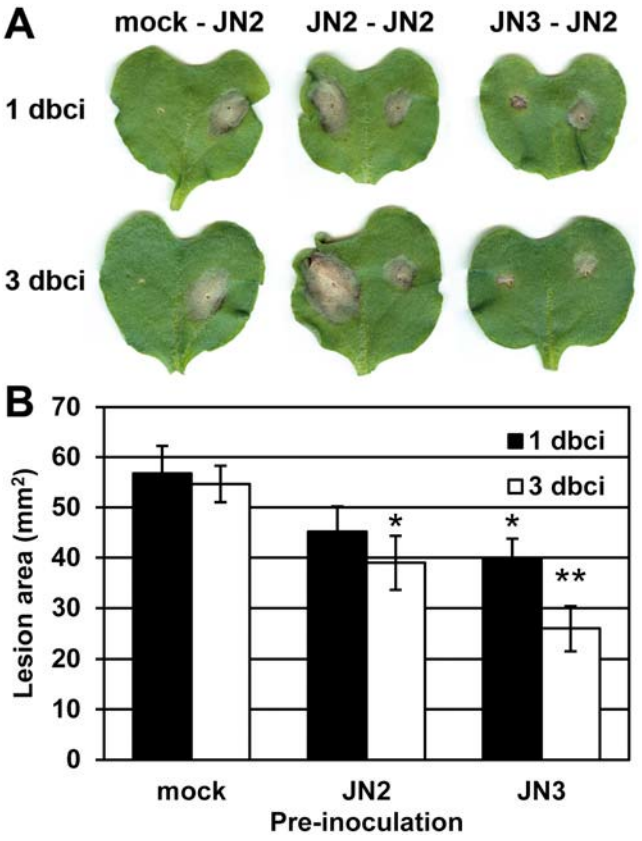

Fig. 3. Resistance induction by preinoculation with *Leptosphaeria maculans* in *Brassica napus* 'Columbus'. At 1 or 3 days before challenge inoculation (dbci), one-half of a cotyledon was puncture inoculated with water (mock) or spore suspension (10^6/ml) of virulent isolate JN2 or avirulent isolate JN3. The opposite half of the cotyledon was subsequently challenge inoculated with JN2. **A,** Typical cotyledons showing lesions caused by preinoculation (left lobe) and challenge inoculation (right lobe). **B,** Area of lesion caused by challenge inoculation was measured using image analysis. Values represent means ± standard error from 20 cotyledons. Asterisks indicate statistically significant differences compared with mock preinoculation (* and ** indicate $P < 0.05$ and 0.01, respectively; Student's *t* test). The experiment was repeated twice, with similar results.

tion. Thus, we inoculated both isolates onto plants of susceptible *B. napus* 'Westar' lacking the *Rlm1* gene. Cotyledons of Westar showed no differences in symptoms caused by JN2 or JN3 (Fig. 1B). Both isolates caused large lesions and their mycelium colonized the tissue intensively. The amount of fungal DNA in Westar cotyledons was precisely quantified by quantitative (q)PCR at 7 DAI. Once more, we saw no difference between JN2 and JN3 (Fig. 2B).

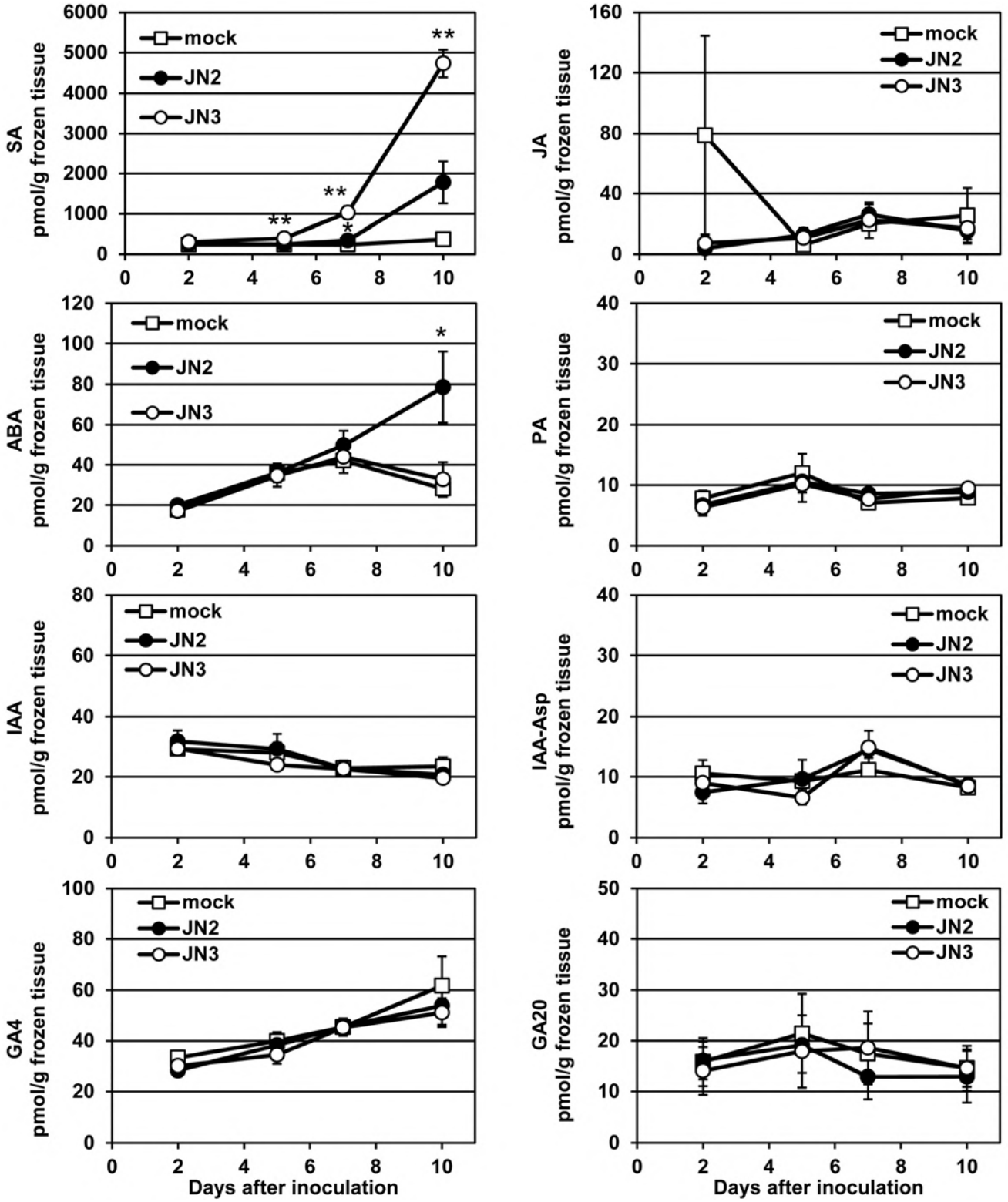

Fig. 4. Liquid chromatography–mass spectrometry analysis of hormone levels in *Brassica napus* 'Columbus' infected with *Leptosphaeria maculans* virulent isolate JN2 and avirulent isolate JN3. Abscisic acid (ABA) and its catabolic product, phaseic acid (PA); indole-3-acetic acid (IAA) and its inactive conjugate, IAA-aspartate (IAA-Asp); salicylic acid (SA); jasmonic acid (JA); gibberellin 4 (GA4); and gibberellin 20 (GA20) were determined in extracts from cotyledons. Plants (11 days old) were inoculated by infiltration of spore suspension (10^5/ml). Control plants were infiltrated with water (mock). Values represent means ± standard error from three independent experiments. Asterisks indicate statistically significant differences compared with mock inoculation (* and ** indicate $P < 0.05$ and 0.01, respectively; Student's *t* test).

The difference in growth between JN2 and JN3 on the *Rlm1* Columbus was accurately quantified by a reverse-transcriptase (RT)-qPCR expression analysis of *L. maculans*'*s* constitutively expressed *LmITS1*. By this approach, the quantification was performed with the same cDNA samples that were used for expression analysis of defense-related marker genes. In in vitro fungal cultures, *LmITS1* was expressed at the same level in JN2 and JN3 when normalized to the expression of *L. maculans Actin* or *Tubulin* (data not shown); thus, the quantity of the transcript in infected cotyledons correlates with fungal mass. In plants, the quantity of *LmITS1* was normalized to the expression of plant *Actin*. We observed the onset of growth for both isolates after 2 DAI (Fig. 2A). Both fungi grew steadily during the 10 days of the experiment but JN2 grew significantly faster. Seven days after inoculation, the quantity of *LmITS1* transcript was four times higher in JN2-infected plants than in JN3-infected ones. Afterward, JN2 continued to grow exponentially whereas the growth rate of JN3 declined. During the 10 days of infection, the mass of JN2 multiplied 16,000 times, whereas JN3 multiplied only 600 times. At 10 DAI, the ratio between the two isolates increased to 27.

We were interested to learn whether defense responses triggered during incompatible interaction with JN3 could restrict subsequent infection by JN2. Hence, we did a puncture inoculation on one lobe of a cotyledon with JN2, JN3, or water and, subsequently, challenge inoculated the opposite lobe of the cotyledon with JN2. Formation of lesions caused by the challenge inoculation was monitored to quantify any effect triggered by a preinoculating agent. Preinoculation of cotyledons with JN3 3 days before challenge inoculation resulted in a more than 50% reduction of lesion size compared with plants preinoculated with water (Fig. 3). This effect was weaker but still significant when the challenge inoculation followed 1 day after preinoculation. Interestingly, preinoculation with JN2 also reduced symptoms caused by challenge inoculation with JN2 (Fig. 3).

Hormone signaling.

Plant responses to pathogens include enhanced synthesis of plant hormones (Pieterse et al. 2009). We wanted to know if the synthesis of any hormone is affected by the recognition of *AvrLm1*. Using liquid chromatography–mass spectrometry (LC-MS), we measured simultaneously levels of abscissic acid (ABA) and its catabolic product, phaseic acid (PA); indole-3-acetic acid (IAA) and its inactive conjugate, IAA-aspartate; SA; JA; gibberellin 4; and gibberellin 20 during the first 10 days of infection by JN2 and JN3. We did not analyze hormone levels after 10 DAI because, from day 11 onward, necrotic lesions appeared on JN2-infected plants and led to cotyledon death (Fig. 1). The levels of most hormones remained unaffected by the infection (Fig. 4). SA production, however, was significantly induced by the avirulent isolate JN3 from

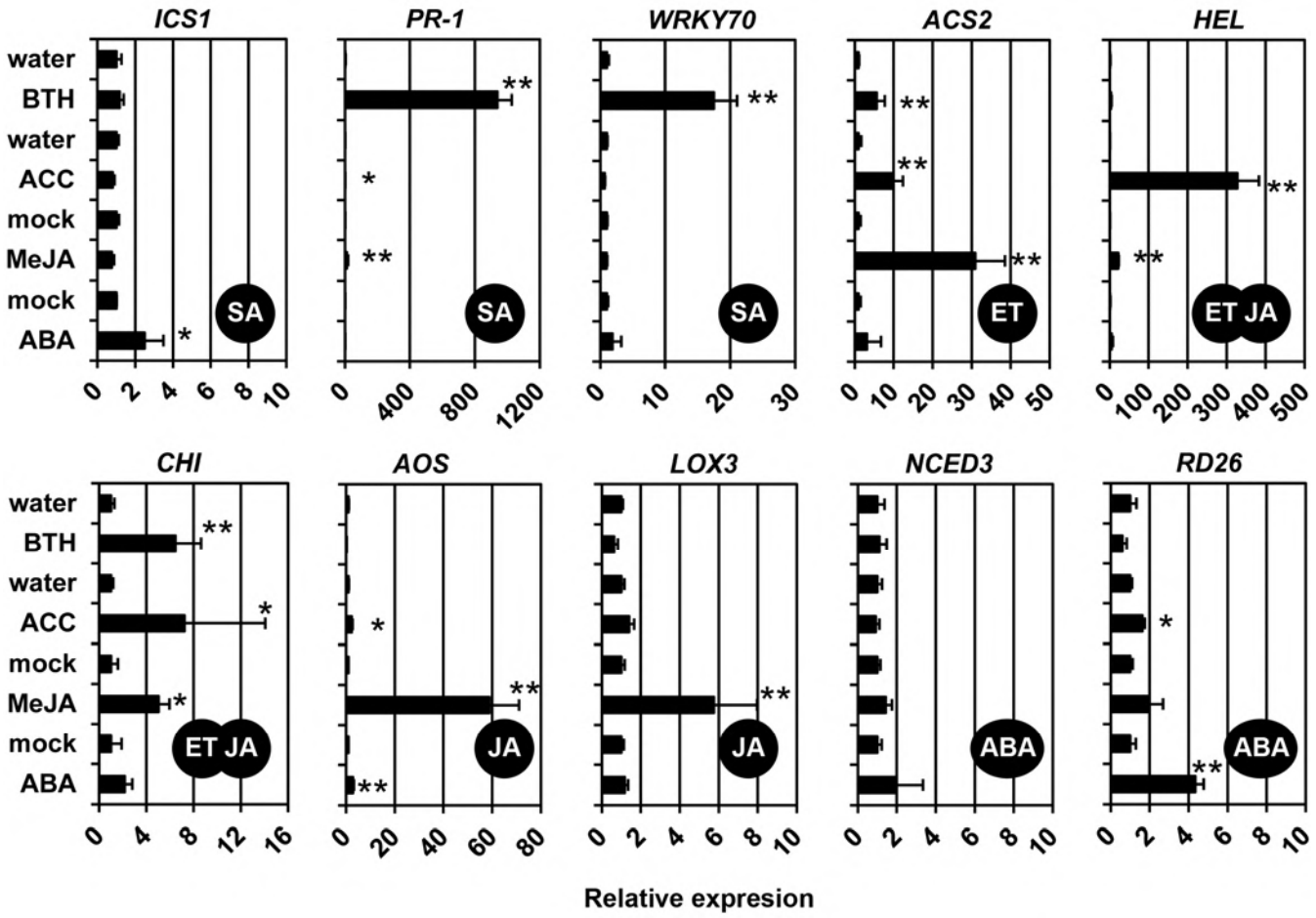

Fig. 5. Validation of salicylic acid (SA), ethylene (ET), jasmonic acid (JA), and abscisic acid (ABA) marker genes in *Brassica napus*. Reverse-transcription quantitative polymerase chain reaction expression analysis was performed 24 h after chemical induction. Seedlings (14 days old) were sprayed with water, SA functional analogue 32 µM benzothiadiazole (BTH), or ET precursor 5 mM 1-aminocyclopropane-1-carboxylic acid (ACC) or plants were incubated in an airtight container in an atmosphere of methyl jasmonate (MeJA). Abscisic acid (ABA) was applied as a 250-µM root drench. Values represent means ± standard error from three independent experiments. Asterisks indicate statistically significant differences compared with the particular control (* and ** indicate $P < 0.05$ and 0.01, respectively; Student's *t* test).

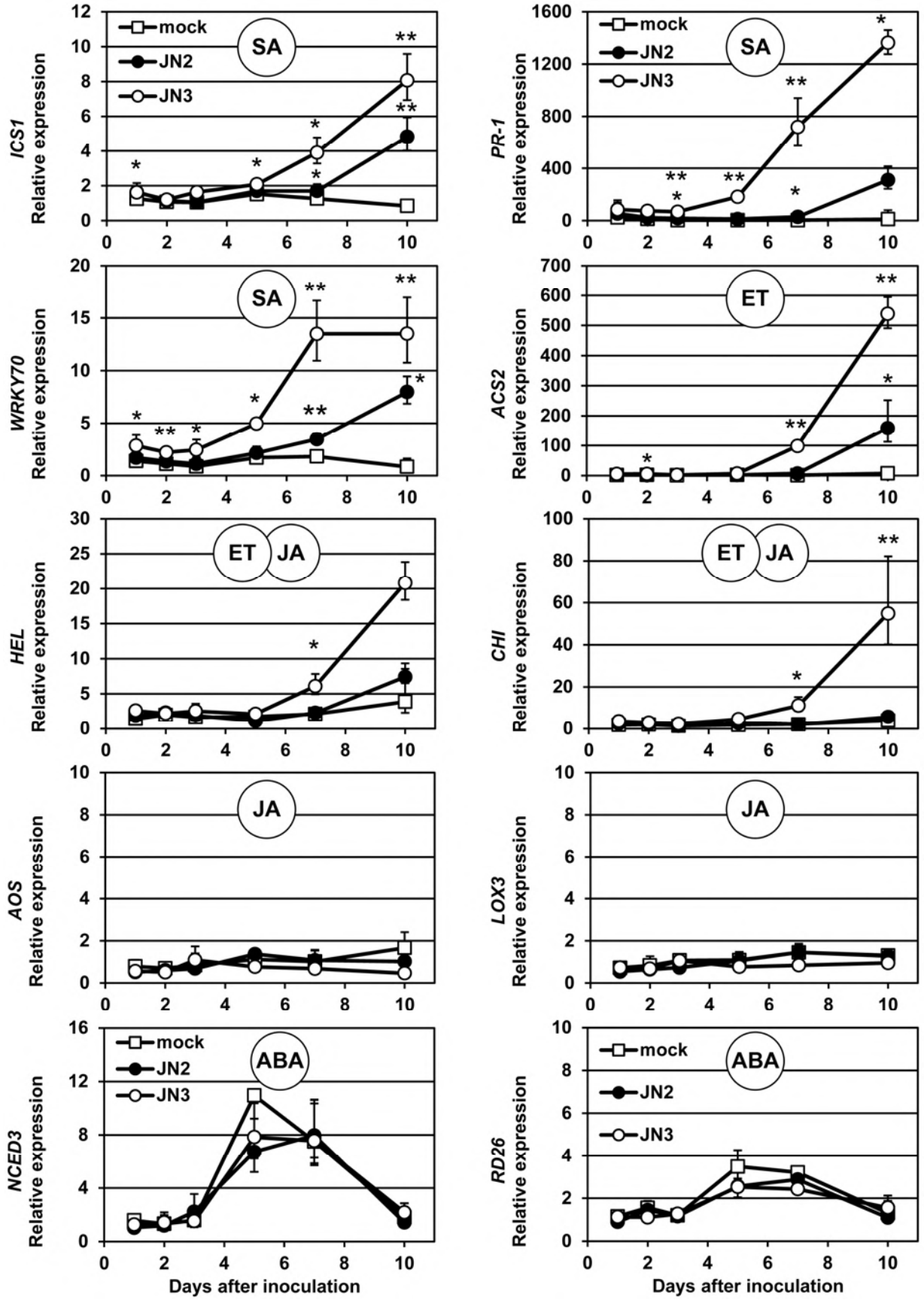

Fig. 6. Expression of salicylic acid (SA), ethylene (ET), jasmonic acid (JA), and abscisic acid (ABA) marker genes in *Brassica napus* 'Columbus' infected with *Leptosphaeria maculans* virulent isolate JN2 and avirulent isolate JN3 determined by reverse-transcription quantitative polymerase chain reaction. Plants (11 days old) were inoculated by infiltration of spore suspension into intercellular space (10^5/ml). Control plants were infiltrated with water (mock). Values represent means ± standard error from three independent experiments. Asterisks indicate statistically significant differences compared with mock-inoculated plants (* and ** indicate $P < 0.05$ and 0.01, respectively; Student's *t* test).

day 5 onward. Its level rose rapidly up to day 10, when it was 13 times higher compared with that in mock-inoculated plants. Although SA was also induced by the virulent isolate JN2, this occurred later and to a smaller degree than in the case of JN3 (Fig. 4). The only other hormone whose level changed during the experiment was ABA. Its concentration rose during the first 7 days of sampling in all plants including controls. The 10-DAI ABA level dropped in mock- and JN3-inoculated plants but increased significantly in plants infected by virulent isolate JN2.

Using RT-qPCR, we sought further to elucidate the role of plant hormones in signaling after the *AvrLm1* gene was recognized. Results of hormone quantification prompted us to investigate the expression of SA-related genes in infected plants. Moreover, we also included ET-, JA-, and ABA-signaling pathways in our study because these hormones have an extreme impact on plant defense response (Pieterse et al. 2009). Because only a few suitable genes have been annotated in *B. napus*, we had to identify new markers for SA-, ET-, JA-, and ABA-signaling pathways. We browsed the *B. napus* expressed sequence tag (EST) database for orthologs of well-characterized marker genes from *A. thaliana*. This approach enabled us to find homologous sequences for most of the selected genes. To confirm the identity of *B. napus* orthologs, expression of each marker gene was analyzed after treatment with the SA functional analogue BTH; ET precursor 1-aminocyclopropane-1-carboxylic acid (ACC); methyl jasmonate (MeJA), a compound that is metabolized in plants to the active form of JA; and, finally, plants were also treated with ABA.

As markers for the SA signaling pathway, we chose *ISOCHORISMATE SYNTHASE 1* (*ICS1*), *PATHOGENESIS-RELATED GENE 1* (*PR-1*), and *WRKY70. ICS1* is the gene involved in SA synthesis following pathogen recognition. Its expression is induced by SA-inducing pathogens but it is not regulated by SA itself (Wildermuth et al. 2001). We identified EST EV225528 as an *ICS1* ortholog in *B. napus*. As with *Arabidopsis*, BTH does not induce *ICS1* expression in *B. napus* (Fig. 5). The only treatment that increased expression of *ICS1* was ABA. *PR-1* is a widely used SA-responsive marker gene in *Arabidopsis,* although its function remains obscure. Its sequence (BNU21849) in *B. napus* was published by Hanfrey and associates (1996). As expected, BTH strongly induced *PR-1* expression in *B. napus* (Fig. 5). ACC and MeJA also significantly increased its expression but the fold change was negligible compared with BTH. *WRKY70* is an SA-responsive transcription factor (Li et al. 2004). Its homologous EST EV113862 in *B. napus* was significantly and specifically induced only by BTH (Fig. 5).

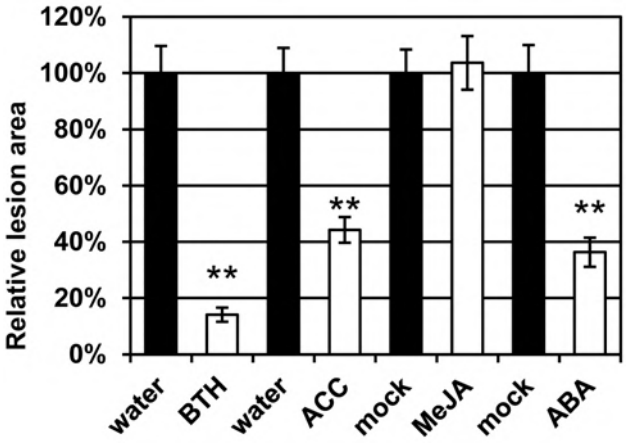

Fig. 7. Resistance induction by pretreatment with inducers of defense signaling pathways. *Brassica napus* 'Columbus' seedlings (11 days old) were sprayed with water, salicylic acid functional analogue 32 μM benzothiadiazole (BTH), or ethylene precursor 5 mM 1-aminocyclopropane-1-carboxylic acid (ACC) or plants were incubated in an airtight container in an atmosphere of methyl jasmonate (MeJA). Abscisic acid (ABA) was applied as a 250-μM root drench. Three days later, cotyledons were inoculated by infiltration with spore suspension (10^5/ml) of *Leptosphaeria maculans* virulent isolate JN2. Area of lesion relative to total cotyledon area was measured using image analysis. Values represent means ± standard error from 24 cotyledons. The mean of each control treatment was set to 100%. Asterisks indicate statistically significant differences compared with control treatment (** indicates $P < 0.01$, Student's t test). The experiments were performed at least three times with similar results.

1-AMINO-CYCLOPROPANE-1-CARBOXYLATE SYNTHASE 2 (*ACS2*) was chosen as a marker gene for ET signaling. It is coding for the ACC synthase, the key enzyme in ET biosynthesis. Expression of *ACS2* is induced during interaction with various pathogens in *Arabidopsis* (Broekaert et al. 2006). We found no suitable ortholog of *ACS2* in the *B. napus* EST database. Using a combination of primers designed to conserved regions of *ACS2,* we amplified a 1-kb product from the cDNA of *B. napus* plants infected by *L. maculans*. An analysis of sequencing data yielded two distinct sequences sharing 95% identity. The genes were named *Bna.X.ACS.a* and *Bna.X.ACS.b* and submitted to GenBank under accession numbers HM450312 and HM450313, respectively. The transcripts of both *B. napus ACS2* genes were present at a very low copy number in noninfected plants. Therefore, the amount of template and annealing time in the qPCR had to be increased. Inasmuch as both genes were similarly induced by *L. maculans* (data not shown), only *Bna.X.ACS.a* (*ACS2a*) was used for subsequent investigations. We observed its enhanced expression after treatment with BTH, ACC, and MeJA (Fig. 5). This fact could complicate the interpretation of results obtained from *ACS2a* expression analysis. However, because ACS operates upstream of ET production and enhanced expression of ACS genes correlates with ET induction (Argueso et al. 2007), increased expression of *ACS2a* indicates activation of ET signaling. The two remaining genes, *HEL* (also described as *PR-4*) and chitinase (*CHI*), are concomitantly regulated by ET and JA in *Arabidopsis* (Norman-Setterblad et al. 2000). We identified *HEL* homologous EST FG577475 in *B. napus*. The *CHI* gene (X61488) used in this study was cloned originally from a *B. napus* cultivar resistant to *L. maculans* (Rasmussen et al. 1992).

As in *Arabidopsis*, both genes were induced in *B. napus* after treatment with ACC and MeJA (Fig. 5). In addition, *CHI* was also induced by BTH and, thus, has an expression profile similar to that of *ACS2*. *ALLENE OXIDE SYNTHASE (AOS*) and *LOX3* were selected as JA-signaling markers. The *AOS* gene is involved in the biosynthesis of JA, and its expression is induced by JA via a positive feedback loop (Laudert and Weiler 1998). *LOX3,* as a member of the lipoxygenase gene family, also participates in JA synthesis (Caldelari et al. 2011). The homologous genes in *B. napus* were identified as EV124323 (*AOS*) and EV113862 (*LOX3*). Congruent with *Arabidopsis*, both genes were strongly induced by MeJA treatment (Fig. 5). *AOS* was also induced by ACC and ABA but only slightly in comparison with MeJA.

As markers for the ABA signaling pathway, we chose *NCED3* and *RD26. NCED3* is a key enzyme of ABA biosynthesis (Iuchi et al. 2001). Its corresponding EST in *B. napus* was identified as EV137674. Expression of *NCED3* was not affected by any of the treatments (Fig. 5). The fact that the EST corresponds to real *NCED3* is supported by a clear correlation between the changes in ABA levels caused by environmental conditions (Fig. 4) and expression of the gene (Fig. 6). *RD26* is a commonly used marker whose expression is regulated by ABA (Fujita et al. 2004). We identified its ortholog as GT085050. As expected, the gene was induced by ABA (Fig. 5). As in *Arabidopsis, RD26* was also induced slightly by ACC.

Using the set of characterized marker genes, we analyzed hormone signaling in *B. napus* infected by JN2 and JN3. Plants were sampled at six time points from 1 to 10 DAI. All three SA marker genes were induced by both isolates (Fig. 6). During a compatible interaction with virulent isolate JN2, expression of *WRKY70* and *PR1* first became apparent at 7 DAI. *ICS1* was significantly induced first at 10 DAI. In stark contrast, JN3 induced *WRKY70* and *ICS1* as early as 24 h after inoculation and the expression of these marker genes together with *PR-1* rose dramatically from 5 DAI. Expression of *ICS1*, *PR-1*, and *WRKY70* reached significantly higher levels than was observed for JN2. Thus, the recognition of *AvrLm1* resulted in a strong induction of SA-associated genes. Unexpectedly, the ET marker gene *ACS2* together with ET/JA markers *HEL* and *CHI* also were strongly induced by JN3 (Fig. 6). The increases in gene expression of the three marker genes were comparable with those observed for SA markers but appeared later, at 7 DAI. JN2 induced only *ACS2a* at 10 DAI and to a moderate level. Therefore, induction of these genes is more specific to *AvrLm1* than is the expression of SA markers. In accordance with the results of hormone quantification (Fig. 4), the expression of both JA markers was unaffected by the infection (Fig. 6). The expression of the ABA marker correlated with ABA levels in that *NCED3* and *RD26* increased their expression of up to 7 DAI in all plants, including the controls, and then decreased. This profile correlates well with the level of ABA (Fig. 4). However, we did not detect any increase of expression in JN2-infected plants at 10 DAI, as was observed for the ABA level (Fig. 6).

Activation of any signaling pathway should not be attributed automatically to plant defense response. Many pathogens have been shown to manipulate plant hormone signaling so as to promote infection (Bari and Jones 2009). Using a pharmacological approach, we investigated the roles of SA-, ET-, JA-, and ABA-signaling pathways in the *B. napus–L. maculans* interaction. Plants were treated with BTH, ACC, MeJA, or ABA under the same conditions used for marker gene profiling and, subsequently, inoculating them with virulent isolate JN2. Lesions caused by the pathogen were measured using image analysis and the effect of each treatment was evaluated. Activation of SA-, ET-, and ABA-signaling pathways by BTH, ACC, and ABA, respectively, resulted in a significant reduction of

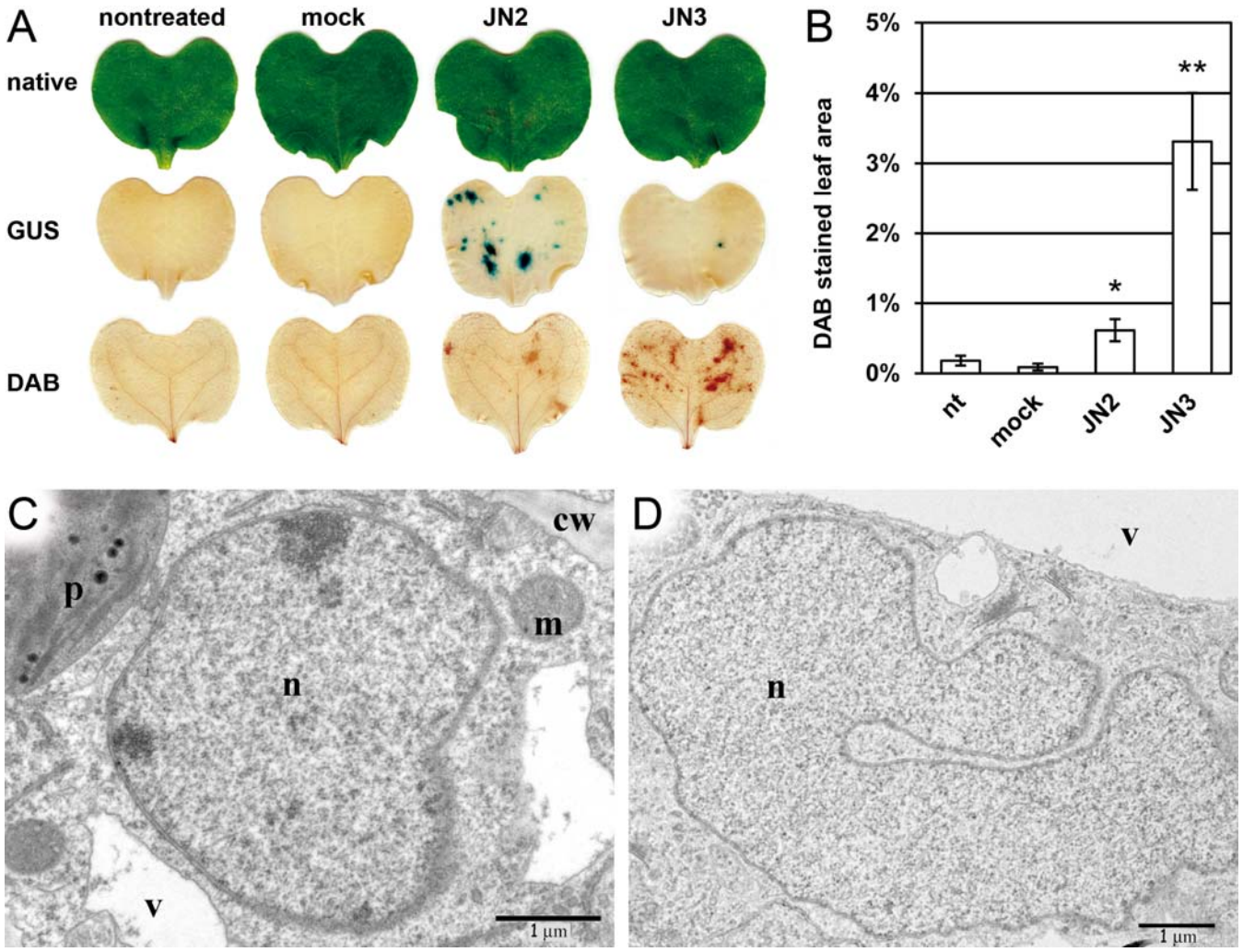

Fig. 8. A, Detection of hydrogen peroxide in *Brassica napus* 'Columbus' cotyledons infected with *Leptosphaeria maculans* virulent isolate JN2 and avirulent isolate JN3. Plants were inoculated by infiltration of spore suspension (10^5/ml). Control plants were infiltrated with water (mock). Eight days after inoculation, hydrogen peroxide was detected in situ by diaminobenzidine (DAB) staining. At the same time, mycelium was visualized by β-glucuronidase (GUS) staining. **B,** DAB-stained area relative to total cotyledon area was measured using image analysis. Values represent means ± standard error from 20 cotyledons. Asterisks indicate statistically significant differences compared with mock-inoculated plants (* and ** indicate $P < 0.05$ and 0.01, respectively; Student's *t* test). The experiment was performed three times with similar results. **C** and **D,** Cytology of infected tissue investigated by transmission electron microscopy. **C,** Nuclei from cells near lesions caused by virulent isolate JN2 show normal morphology. **D,** Invaginations of nuclear membrane in cells near lesions caused by avirulent isolate JN3. Legend: cw, cell wall; m, mitochondrion; n, nucleus; p, plastid; v, vacuole.

disease symptoms (Fig. 7). Treatment by ACC and ABA was less efficient than it was with BTH. Disease symptoms caused by JN2 on cotyledons pretreated with BTH resembled those formed on nontreated cotyledons infected by JN3 (data not shown). Such lesions were small, dark, and deeply embedded in the tissue. Treatment with MeJA had no effect on disease progression (Fig. 7).

Production of hydrogen peroxide and callose deposition.

Recognition of avirulent pathogens often triggers enhanced production of ROS in the surrounding tissue (Torres et al. 2006). We monitored the formation of hydrogen peroxide for 10 days following inoculation with JN2 and JN3 using diaminobenzidine (DAB) staining. No cotyledons showed staining during the early stage of infection (data not shown). At 8 DAI, we observed intensive and localized staining of hydrogen peroxide in cotyledons infected by JN3. By contrast, JN2-infected cotyledons showed only weak and diffuse staining (Fig. 8A). The intensively stained area was five times larger in cotyledons infected by JN3 than in those infected by JN2 (Fig. 8B). To link the hydrogen peroxide production with the actual state of infection, we visualized the mycelium by GUS staining. At 8 DAI, most cotyledons exhibited no symptoms at all (Fig. 8A). Only a few JN2-infected cotyledons showed small areas of collapsing tissue. Whereas GUS-stained mycelium of JN3 appeared only as a few tiny spots, cotyledons infected by JN2 showed several spreading stains. Furthermore, we analyzed expression of NADPH-oxidase genes in response to infection. The orthologs to *Arabidopsis rbohC, rbohD*, and *rbohF* genes were identified in the *B. napus* EST database. Nevertheless, expression of all three genes was unaffected by infection (Supplementary Fig. S1).

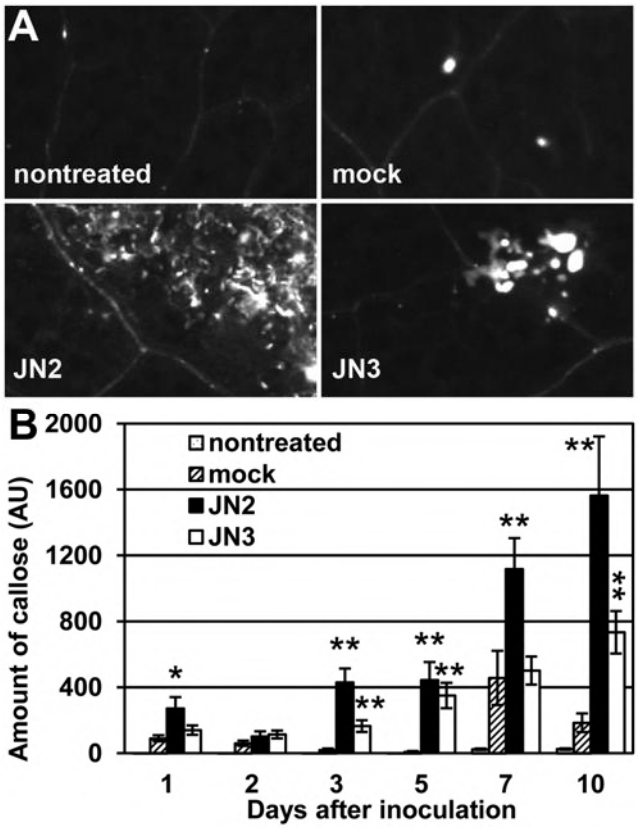

Fig. 9. Callose deposition in *Brassica napus* 'Columbus' cotyledons infected with *Leptosphaeria maculans* virulent isolate JN2 and avirulent isolate JN3. Plants were inoculated by infiltration of spore suspension (10^5/ml). Control plants were infiltrated with water (mock). Callose was stained by aniline blue and observed with fluorescent microscopy. **A,** Typical pictures of stained cotyledon tissue 10 days after inoculation under ×200 magnification. Callose stained with aniline blue displays bright fluorescence. **B,** Bright area of each picture was measured using image analysis. Values represent means ± standard error from 40 pictures taken randomly from 10 plants. Asterisks indicate statistically significant differences compared with mock inoculation (* and ** indicate $P < 0.05$ and 0.01, respectively; Student's *t* test). Similar results were observed in three experiments.

Using transmission electron microscopy, we investigated the cytology of tissue infected by JN2 and JN3. Plants were puncture inoculated to localize the infection. Samples were collected at 6 DAI. At that time, the puncture was surrounded by a zone of dying tissue. This zone was larger in JN2-inoculated cotyledons. Electron microscopic observations of cells in this zone revealed a different cytological response in compatible versus incompatible interaction. Whereas nearly intact nuclei with a rounded nuclear envelope were found in JN2-infected plants (Fig. 8C), cells of plants infected by JN3 showed altered nuclear morphology. Large invaginations of the nuclear membrane were characteristic (Fig. 8D).

Plants reinforce their cell walls at the sites of pathogen attack as a part of their defense strategy. One of the most abundant compounds deposited into newly formed barriers is the polysaccharide callose (Hématy et al. 2009). Callose is required for resistance against *L. maculans* in *Arabidopsis* (Staal et al. 2006). Using aniline blue staining, we quantified the deposition of callose in plants infected by JN2 and JN3 to decipher its involvement in *AvrLm1*-triggered responses (Fig. 9A). We observed intensive callose deposition from 3 DAI in plants infected by both isolates (Fig. 9B). The amount of callose increased in time but, in stark contrast to the SA synthesis, marker gene expression, or hydrogen peroxide, we always detected more callose in plants infected by JN2 than by JN3. Although the staining was localized to relatively small areas in JN3-infected cotyledons, it displayed stronger intensity compared with tissue infected by JN2 (Fig. 9A).

DISCUSSION

We have shown that *B. napus* carrying *Rlm1* responds to *AvrLm1* by activating several defense mechanisms that result in a dramatic difference in tissue colonization between the virulent and avirulent isolates (Figs. 1 and 2). The growth restriction of the avirulent isolate clearly can be attributed to the *AvrLm1* and not to another genetic background because no difference in tissue colonization could be observed between JN2 and JN3 on plants lacking the *Rlm1* gene (Figs. 1 and 2). *AvrLm1* restricts the fungal growth through activation of plant defenses. Preinoculation of plants with an avirulent isolate reduces the colonization of a virulent isolate (Fig 3). This cannot be explained by mere nutriental exploitation from the preinoculating pathogen because JN3 caused only slight damage to the cotyledon in comparison with JN2 but was still more efficient in protecting plants from the challenging pathogen. The longer time span between pre- and challenge inoculation increases the effect, indicating the need for a certain time period to fully activate the defense machinery. We demonstrated the existence of at least partially systemic signaling triggered by *AvrLm1* because the challenge inoculation was performed on the opposite lobe of the cotyledon (Fig. 3). The *AvrLm1–Rlm1* interaction has some typical features of incompatible interaction as known from biotrophic pathogens. The avirulent isolate caused symptoms resembling macroscopic HR, and a cytological hallmark of HR in the form of lobed nuclei at 6 DAI were also detected (Fig. 8). Similar observations had been reported earlier for incompatible interaction of *B. napus* with *L. maculans* (Roussel et al. 1999). We also detected production of hydrogen peroxide triggered by *AvrLm1* at 8 DAI (Fig. 8). It is generally believed

that an oxidative burst is an early plant response to pathogens preceding the HR (Mur et al. 2008). In fact, in our experiments, production of hydrogen peroxide appeared later than induction of the SA-signaling pathway, which had been thought to be a late response. Yet the DAB staining does not seem sufficiently sensitive to detect early accumulation of hydrogen peroxide (Pellinen et al. 2002).

SA and ET interplay during *AvrLm1* recognition.

We found that recognition of *AvrLm1* triggers the biosynthesis of SA in infected plants (Fig. 4) and expression of the SA marker genes *ICS1*, *PR-1*, and *WRKY70* (Fig. 6). A positive role of SA in mediating resistance to *L. maculans* was proven by an inoculation test. The treatment of plants with the SA functional analogue BTH reduced the size of the lesion caused by the virulent isolate (Fig. 7). This result confirmed conclusions as to the indispensable role of SA in *B. napus* resistance to *L. maculans* stated by Potlakayala and associates (2007). The plants had responded to *AvrLm1* as early as 1 DAI by induction of the SA markers *ICS1* and *WRKY70*. At that point, spores of *L. maculans* are just germinating and expression of *AvrLm1* is very low (Fudal et al. 2007). Consequently, mechanisms recognizing AvrLm1 or its effect must be extremely sensitive. The early exposure of the AvrLm1 protein to plant recognition mechanisms indicates its possible role in early infection events.

In addition to SA-signaling activation, we also observed induction of the ET biosynthesis gene *ACS2a* and two marker genes (*HEL* and *CHI*) responsive to ET and JA after infection with the avirulent isolate. Because expression of the JA markers *AOS* and *LOX3* (Fig. 6) as well as JA content (Fig. 4) remained unaffected, we concluded that induction of *HEL* and *CHI* was the result of enhanced ET biosynthesis. As with SA, chemical induction of the ET-signaling pathway increased the resistance to *L. maculans* (Fig. 7). That provides additional evidence of ET involvement in defense responses triggered by *AvrLm1*. In comparison with SA signaling, expression of ET markers increased later, at 7 DAI, and responded only slightly to the virulent isolate (Fig. 6). Interestingly, the growth rate of the avirulent isolate declined after 7 DAI (Fig 2 A). This relationship indicates that ET might, in addition to SA, be a key element necessary for growth restriction of the avirulent isolate.

SA is a key regulator of defense responses effective against biotrophs in several plant species and is also essential for *R* gene–mediated resistance (Vlot et al. 2009). The role of ET in plant responses is less clear, however. ET influences disease development either positively or negatively depending on the particular plant–pathogen interaction. In *Arabidopsis*, ET simultaneously with JA regulates defense responses that are effective against necrotrophs. ET and JA pathways act at least independently or even antagonistically with respect to the SA pathway (Broekaert et al. 2006). Thus, the simultaneous activation of SA and ET signaling pathways after *AvrLm1* recognition observed in our experiments is an atypical event. Nevertheless, it has been reported in several instances. Tomato plants were shown to produce high levels of ET and SA during interaction with *Cladosporium fulvum* Avr proteins Avr2 and Avr9 (Hammond-Kosack and Jones 1996). Silencing of *Nicotiana benthamiana ICS1* and *EIN2*, key elements of SA and ET signaling pathways, respectively, resulted in enhanced susceptibility to *Phytophthora infestans*, whereas silencing of the key JA regulator *COI1* had no effect on resistance (Shibata et al. 2010). Functional SA and ET signaling was necessary for *Arabidopsis* resistance to *Colletotrichum higginsianum* (Liu et al. 2007). Interestingly, these three pathogens are facultative parasites with an initial asymptomatic phase of infection followed by lesion formation. One can assume that simultaneous activation of SA and ET signaling is a response of plants to the contrasting stages of infection. The increase in expression of ET marker genes observed at 7 DAI during an incompatible interaction with JN3 (Fig. 6) coincides with the onset of necrotrophic behavior. The first macroscopically visible necrosis appeared just after the strongest expression was detected at 10 DAI (Fig. 1).

B. napus plants also responded to infection by the virulent isolate. It is noteworthy that, although the defense responses during compatible interaction differed largely by timing and magnitude, they were qualitatively similar to those triggered by the recognition of *AvrLm1*. The qualitative similarities between compatible and incompatible interaction are frequently observed but the basis of this phenomenon is unknown (Tao et al. 2003). How can *AvrLm1*-induced responses be similar to those observed during compatible interaction? The most likely explanation is that the activation of SA and ET signaling pathways could be an outcome from recognition of *L. maculans*-associated molecules. A virulent isolate will be capable of suppressing the defense signaling by its large array of effectors. Recognition of *AvrLm1* will bypass the suppressed signaling nodes and reactivate the SA and ET signaling. The latter hypothesis is supported by the conclusions of Lee and associates (2009). Their "repair" model proposes that basal resistance and *R* gene–mediated resistance are not separate entities. Instead, activation of the *R* gene restores the normal function of basal resistance that was impaired by the action of pathogen effectors.

Resistance to *L. maculans* is mediated differently in *B. napus* and *Arabidopsis*.

Our findings concerning the crucial role of SA and ET in resistance of *B. napus* to *L. maculans* are in stark contrast to what is known about resistance mechanisms in *Arabidopsis*. There, functional SA signaling is not required for resistance, and ET signaling probably influences plant defense negatively (Persson et al. 2009). Although resistance in *B. napus* was not associated with heightened ABA levels in our study (Fig. 4), increase in ABA level has been observed during incompatible interaction of *L. maculans* with *Arabidopsis* and ABA signaling has been shown to mediate phenotype resistance (Kaliff et al. 2007). Incompatible interaction in *Arabidopsis* is associated with enhanced callose deposition (Staal et al. 2006). In our experiments with *B. napus*, we consistently observed more callose deposition in those tissues infected by a virulent isolate than by an avirulent one (Fig. 9). Our conclusions are based mainly on the results of pharmacological experiments and gene expression analysis while most findings regarding *Arabidopsis* were reached by genetic approaches using mutants impaired in particular defense responses. Nevertheless, it seems obvious that the defense mechanisms against *L. maculans* are different in the two plant species. This finding was unanticipated because *Arabidopsis* and *B. napus* belong to the Brassicaceae family. The importance of the JA pathway for *Arabidopsis* resistance to *L. maculans* indicates that the plants activate defenses effective against necrotrophs. Compared with *B. napus* (Fig. 2), the susceptible genotypes of *Arabidopsis* allow only very slow colonization by the fungus (Persson et al. 2009). It is possible that the biotrophic phase in *Arabidopsis* could be reduced and the fungus is forced to grow as a necrotroph.

Grouping of fungal pathogens based on their infection strategy is often arguable because no distinct borders exist between necrotrophs and biotrophs (Oliver and Solomon 2010). Here, we show that the same fungal pathogen can interact in a completely different way with two related plant species. This underscores the need for studies conducted on natural hosts and to not rely only on data obtained from model systems.

MATERIALS AND METHODS

Plant and pathogen cultivation.

B. napus plants were grown in perlite nourished with Steiner's nutrient solution (Steiner 1984) in a cycle of 14 h of day (150 μE m^{-2} s^{-1}, 24°C) and 10 h of night (19°C) at 65% relative humidity. True leaves were removed once or twice in plants cultivated longer than 2 weeks to avoid cotyledon senescence. With plants assayed for defenses to *L. maculans,* leaves were removed once at 7 DAI. *L. maculans* isolates JN2 and JN3, also referred to as v23.1.2 and 23.1.3, respectively (Balesdent et al. 2002), were cultivated on V8 juice agar at 24°C in the dark. Sporulation was done according to Ansan-Melayah and associates (1995). Spores were washed once with distilled water after harvesting, diluted to 10^8 spores/ml, and stored at –20°C for a maximum period of 6 months. Plants were inoculated either by infiltration of spore suspension (10^5 spores/ml) into the cotyledon using a 1-ml plastic syringe or by placing 10 μl of spore suspension (10^6 spores/ml) on a cotyledon that was punctured by a sterile needle. All experiments were performed using GUS-tagged isolates.

Transformation of *L. maculans* with GUS.

L. maculans isolates JN2 and JN3 were transformed with a pSO1 construct (Persson et al. 2009) carrying the GUS gene, according to Gardiner and Howlett (2004). Transformants were assessed for GUS staining in vitro and compared with wild-type isolates for virulence to exclude possible alterations caused by transformation. In the selected lines, the presence or absence of *AvrLm1* was confirmed by PCR. The Fast Tissue-to-PCR Kit (Fermentas, Vilnius, Lithuania) was used for PCR, with 1.5×10^8 spores pelleted and used as a template for the PCR. The following PCR program was used: 95°C for 3 min, followed by 35 cycles of 95°C for 30 s, 55°C for 30 s, and 72°C for 30 s. Amplification of *Tubulin* was used as a control for equal loading of the DNA template. Primers were used for amplification: *Tubulin*, AY749017, FP: 5′-TCA AGA TGT CCT CCA CCT-3′, RP: 5′-GTA CCA ATG CAA GAA AGC C-3′; *AvrLm1*, AM084345, FP: 5′-TTT AAT CAC GAA GAC AAC CC-3′, RP: 5′-CAC AAC AAA GCA ATA ACG AG-3′.

GUS assay.

Detached cotyledons were immersed in a staining solution (15 mg of 5-bromo-4-chloro-3-indolyl-D-glucuronic acid in 0.6 ml of dimethylformamide; 0.3 ml of 10% Triton-X; 0.6 ml of 0.5 M EDTA, pH 8.0; 3 ml of 5 mM ferrocyanide; 3 ml of 5 mM ferricyanide; and 3 ml of 1 M phosphate buffer, pH 7.0) and infiltrated under vacuum in a six-well plate. Infiltrated cotyledons were incubated at 37°C for several hours until the mycelium became visible. After rinsing with water, the chlorophyll was removed using 96% ethanol. Rehydrated cotyledons were scanned under a transmission light.

Transmission electron microscopy.

Small parts of puncture-inoculated cotyledon tissue sampled near the infection sites were fixed in 2.5% glutaraldehyde in 0.1 M phosphate buffer (pH 7.2) for 3 h. After washing in a 0.1 M phosphate buffer, the tissue pieces were post-fixed for 2 h with 1% osmium tetroxide dissolved in the same buffer. Samples were washed in buffer and dehydrated in a graded ethanol series and propylene oxide, then infiltrated with and embedded in Durcupan epoxy resin. Ultrathin sections (70 nm) were cut with a Reichert Jung Ultracut E ultramicrotome (Reichert-Jung, Vienna) and stained with uranyl acetate (6 min) and lead citrate (6 min). Sections were viewed at 75 kV using a Hitachi 7100 transmission electron microscope (Hitachi, Tokyo).

Treatments with chemicals.

Plants were sprayed with 32 μM BTH (Bion 50 WG; Syngenta, Basel, Switzerland) or with 5 mM ACC (Sigma-Aldrich, St. Louis). Control plants were sprayed with water. Alternatively, plants were placed in a transparent airtight container (20 liters) with cotton swabs containing either 2 μl of MeJA (Sigma-Aldrich) in 18 μl of ethanol or just 18 μl of ethanol as a control. ABA (Sigma-Aldrich) was applied as a root drench; 5 ml of 250 μM ABA in 0.2% ethanol was pipetted to the base of each plant. Control plants were treated with 0.2% ethanol.

Analysis of plant hormones.

Plant hormones were extracted from 150 mg of frozen tissue and determined as previously described (Dobrev and Kaminek 2002; Dobrev et al. 2002) after the addition of appropriate internal standards. Quantitation was done on an Ultimate 3000 high-performance liquid chromatograph (Dionex, Bannockburn, IL, U.S.A.) coupled to a 3200 Q TRAP hybrid triple quadrupole/linear ion trap mass spectrometer (Applied Biosystems, Foster City, CA, U.S.A.).

***ACS2* cloning.**

Partial sequence of putative ACC synthase 2 transcript was amplified from *L. maculans*-infected *B. napus.* The cDNA was prepared according to the same protocol as for gene expression analysis. The fragment was amplified with PCR Master Mix (Promega Corp., Madison, WI, U.S.A.) and primers designed for *B. napus* ESTs homologous to *Arabidopsis ACS2* (FP: TGGATCAAAGAGAACCCAA, RP: CGAAACATTGAGCT TCACTT). The following program was used for PCR: 94°C for 4 min; followed by 30 cycles of 94°C for 10 s, 55°C for 10 s, and 72°C for 30 s; with final extension at 72°C for 5 min. The PCR product was purified using a High Pure PCR cleanup micro kit (Roche, Indianapolis, IN, U.S.A.), cloned into pJET1.2 vector supplied with the CloneJET PCR cloning kit (Fermentas), then sequenced from both ends using pJET1.2 sequencing primers.

Gene expression analysis.

Frozen cotyledons from six plants were ground in liquid nitrogen using mortar and pestle. Total RNA was isolated using a Spectrum Plant Total RNA Kit (Sigma-Aldrich) and treated with a DNA-*free* Kit (Ambion, Austin, TX, U.S.A.). Subsequently, 1 μg of RNA was converted into cDNA with M-MLV RNase H^- Point Mutant reverse transcriptase (Promega Corp.) and anchored oligo dT_{21} primer (Metabion, Martinsried, Germany). An equivalent of 6.25 ng of RNA (25 ng for *ACS2a, NCED3*, and *LmITS1*) was loaded into a 10-μl reaction with a DyNAmo Capillary SYBR Green qPCR Kit (Finnzymes, Vantaa, Finland). All reactions were performed in polycarbonate capillaries (Genaxxon, Ulm, Germany) and LightCycler 1.5 (Roche). The following PCR program was used for all PCR assays: 95°C for 10 min; followed by 45 cycles of 95°C for 10 s, 55°C for 10 s, and 72°C for 10 s; followed by a melting curve analysis. For *ACS2a*, the annealing conditions were modified to 55°C for 20 s and, for *LmITS1*, to 60°C for 20 s. Threshold cycles and melting curves were calculated using LightCycler Software 4.1 (Roche). Relative expression was calculated with efficiency correction and normalization to *Actin*. Primers were designed using PerlPrimer v1.1.17 (Marshall 2004). Following is the list of *B. napus* genes and corresponding accession numbers and primers: *Act,* AF111812, FP: 5′-CTG GAA TTG CTG ACC GTA TGA G-3′, RP: 5′-TGT TGG AAA GTG CTG AGG GA-3′; *ICS1*, EV225528, FP: 5′-CAA ACT CAT CAT CTT CCC TC-3′, RP: 5′-AGC GTG ACT TAC TAA CCA G-3′; *PR-1,* BNU21849, FP: 5′-CAT CCC TCG AAA GCT CAA GAC-3′, RP: 5′-CCA CTG CAC

GGG ACC TAC-3′, *WRKY70*, EV113862, FP: 5′-ACA TAC ATA GGA AAC CAC ACG-3′, RP: 5′-ACT TGG ACT ATC TTC AGA ATG C-3′; *ACS2a,* HM450312, FP: 5′-AGG TGG TCA AAG ACT TAG ATA G-3′, RP: 5′-ACC GAG TCG TTG TAA GAA TA-3′; *HEL*, FG577475, FP: 5′-GGA ACA CAA GGA CTA ATG C-3′, RP: 5′-TTT CGA TAG CCA TCA CCA-3′; *CHI*, X61488, FP: 5′-TGC TAC ATA GAA GAA ATA AAC GG-3′, RP: 5′-TTC CAT GAT AGT TGA ATC GG-3′; *AOS*, EV124323, FP: 5′-CGC CAC CAA AAC AAC AAA G-3′, RP: 5′-GGG AGG AAG GAG AGA GGT TG-3′; *LOX3*, EV113862, FP: 5′-GAA GTT TAT GGC GGT GGT-3′, RP: 5′-CCT GTT TCT ACG GTT AGG A-3′; *NCED3*, EV137674, FP: 5′-CGA TTT GCC TTA CCA AGT CAG-3′, RP: 5′-TTT ATC CCT TCC GGT GAG AA-3′, *RD26,* GT085050, FP: 5′-ATC GGT CTT TCA ATC TTC CT-3′, RP: 5′-GAG TTC ATC TGC AAA TTC CT-3′, *rbohC*, EV222262, FP: 5′-CAA AGA ACA AGC CGA ACT C -3′, RP: 5′-TAA CCC AGT AGA AGT AAG CC-3′, *rbohD*, CB686108, FP: 5′- ACC GTG ATA GTG ACA TAG AG-3′, RP: 5′- ATA ATC CCT TCA TCG TCC AG-3′; and *rbohF*, EV035965, FP: 5′-TGT TCT CTT ATT GGT TGG TC-3′, RP: 5′-TTC CTG TGC TGT TCT CTG-3′. Primers for *LmITS1* (FJ172239) were designed by Persson and associates (2009). All raw qPCR data are presented in Supplementary Table S1.

Quantification of *L. maculans* in cotyledons of *B. napus* Westar.

DNA was extracted from cotyledons using DNAzol (Molecular Research Center, Cincinnati, OH, U.S.A.) following the manufacturer's instructions. DNA (100 ng) was used as a template for a qPCR performed with *LmITS1* and *Act* primers as described in the previous paragraph using the following program: 95°C for 10 min; followed by 45 cycles of 95°C for 10 s, 55°C for 10 s, and 72°C for 10 s; followed by a melting curve analysis. The relative quantity of *LmITS1* was normalized to plant *Actin*. Specificity of *LmITS1* was verified by amplification with DNA from noninoculated plants.

Hydrogen peroxide detection using DAB.

The staining solution was prepared by dissolving 40 mg of DAB (Sigma-Aldrich) in 200 µl of dimethylformamide and mixing it with 40 ml of water. Detached cotyledons were immersed in the staining solution and infiltrated under vacuum. Cotyledons were then kept in a closed petri dish in darkness at room temperature until reddish-brown staining appeared. Chlorophyll was then removed in 96% ethanol, after which cotyledons were rehydrated and scanned in a reflective mode.

Callose staining.

Cotyledon disks (12 mm in diameter) were cut from 10 plants per treatment and stained with aniline blue following the protocol described by Clay and associates (2009), including a clearing step with 10% NaOH. After mounting on slides, the disks were observed with a Leica DM 5000 B fluorescence microscope (Leica, Wetzlar, Germany) using an autofluorescence filter cube (excitation filter 360/40 nm; dichroic mirror; emission filter 470/40 nm). Four pictures were taken at random for each disk and numbers of fluorescing pixels were counted using APS Assess 2.0 image analysis software (The American Phytopathological Society, St. Paul, MN, U.S.A.).

Image analysis and statistics.

The area of lesions caused by *L. maculans* after puncture inoculation was quantified using DPlan4Lab 0.5.1 image analysis software. DAB staining, callose staining, and lesion area caused after spore infiltration were analyzed using APS Assess 2.0 software. During analysis, thresholds were set empirically to obtain optimal detection. Within a given experiment, each object was measured with the same threshold setting to avoid any subjective influence. All statistical analyses were performed using Microsoft Excel 2010. The *P* values were calculated using the two-tailed Student's *t* test. The statistics of expression analysis was performed on log-transformed data.

ACKNOWLEDGMENTS

We thank M. Pařízková and J. Vidláková for their excellent technical support; P. Dobrev for his LC-MS analysis and for numerous discussions with S. Oide and C. Dixelius, who also provided pSO1 plasmid; and T. Rouxel for providing *L. maculans* isolates JN2 and JN3. V. Šašek designed, performed, and analyzed the experiments and also composed the manuscript. M. Nováková designed, performed, and analyzed the experiments dealing with ABA and critically revised the manuscript. B. Jindřichová designed, performed, and analyzed preliminary experiments. K. Bóka designed, performed, and analyzed the experiments dealing with electron microscopy, wrote that particular part of the article, and critically revised the manuscript. O. Valentová created the conception and critically revised the manuscript. L. Burketová created the conception, designed the experiments, and also critically revised the manuscript. All authors concurred in the final version of the manuscript. This research was supported by grants from the Czech Science Foundation (522/08/1581) and the Czech Ministry of Education (MEB040923).

LITERATURE CITED

Ansan-Melayah, D., Balesdent, M. H., Buee, M., and Rouxel, T. 1995. Genetic characterization of *AvrLm1*, the first avirulence gene of *Leptosphaeria maculans*. Phytopathology 85:1525-1529.

Argueso, C. T., Hansen, M., and Kieber, J. J. 2007. Regulation of ethylene biosynthesis. J. Plant Growth Regul. 26:92-105.

Balesdent, M. H., Attard, A., Ansan-Melayah, D., Delourme, R., Renard, M., and Rouxel, T. 2001. Genetic control and host range of avirulence toward *Brassica napus* cultivars Quinta and Jet Neuf in *Leptosphaeria maculans*. Phytopathology 91:70-76.

Balesdent, M. H., Attard, A., Kuhn, A. L., and Rouxel, T. 2002. New avirulence genes in the phytopathogenic fungus *Leptosphaeria maculans*. Phytopathology 92:1122-1133.

Bari, R., and Jones, J. D. 2009. Role of plant hormones in plant defence responses. Plant Mol. Biol. 69:473-488.

Bohman, S., Staal, J., Thomma, B. P., Wang, M., and Dixelius, C. 2004. Characterisation of an *Arabidopsis–Leptosphaeria* maculans pathosystem: Resistance partially requires camalexin biosynthesis and is independent of salicylic acid, ethylene and jasmonic acid signalling. Plant J. 37:9-20.

Broekaert, W. F., Delaure, S. L., De Bolle, M. F. C., and Cammuel, B. P. A. 2006. The role of ethylene in host–pathogen interactions. Annu. Rev. Phytopathol. 44:393-416.

Caldelari, D., Wang, G. G., Farmer, E. E., and Dong, X. N. 2011. Arabidopsis *lox3 lox4* double mutants are male sterile and defective in global proliferative arrest. Plant Mol. Biol. 75:25-33.

Clay, N. K., Adio, A. M., Denoux, C., Jander, G., and Ausubel, F. M. 2009. Glucosinolate metabolites required for an Arabidopsis innate immune response. Science 323:95-101.

Delourme, R., Chèvre, A. M., Brun, H., Rouxel, T., Balesdent, M. H., Dias, J. S., Salisbury, P., Renard, M., and Rimmer, S. R. 2006. Major gene and polygenic resistance to *Leptosphaeria maculans* in oilseed rape (*Brassica napus*). Eur. J. Plant Pathol. 114:41-52.

Dobrev, P. I., and Kaminek, M. 2002. Fast and efficient separation of cytokinins from auxin and abscisic acid and their purification using mixed-mode solid-phase extraction. J. Chromatogr. A 950:21-29.

Dobrev, P., Motyka, V., Gaudinova, A., Malbeck, J., Travnickova, A., Kaminek, M., and Vankova, R. 2002. Transient accumulation of cis- and trans-zeatin type cytokinins and its relation to cytokinin oxidase activity during cell cycle of synchronized tobacco BY-2 cells. Plant Physiol. Biochem. 40:333-337.

Dodds, P. N., and Rathjen, J. P. 2010. Plant immunity: Towards an integrated view of plant-pathogen interactions. Nat. Rev. Genet. 11:539-548.

Fitt, B. D. L., Brun, H., Barbetti, M. J., and Rimmer, S. R. 2006. Worldwide importance of phoma stem canker (*Leptosphaeria maculans* and *L. biglobosa*) on oilseed rape (*Brassica napus*). Eur. J. Plant Pathol. 114:3-15.

Fudal, I., Ross, S., Gout, L., Blaise, F., Kuhn, M. L., Eckert, M.R., Cattolico, L., Bernard-Samain, S., Balesdent, M. H., and Rouxel, T. 2007. Hetero-

chromatin-like regions as ecological niches for avirulence genes in the *Leptosphaeria maculans* genome: Map-based cloning of *AvrLm6*. Mol. Plant-Microbe Interact. 20:459-470.

Fujita, M., Fujita, Y., Maruyama, K., Seki, M., Hiratsu, K., Ohme-Takagi, M., Tran, L.S., Yamaguchi-Shinozaki, K., and Shinozaki, K. 2004. A dehydration-induced NAC protein, RD26, is involved in a novel ABA-dependent stress-signaling pathway. Plant J. 39:863-876.

Gardiner, D. M., and Howlett, B. J. 2004. Negative selection using thymidine kinase increases the efficiency of recovery of transformants with targeted genes in the filamentous fungus *Leptosphaeria maculans*. Curr. Genet. 45:249-255.

Gout, L., Fudal, I., Kuhn, M. L., Blaise, F., Eckert, M., Cattolico, L., Balesdent, M. H., and Rouxel, T. 2006. Lost in the middle of nowhere: The *AvrLm1* avirulence gene of the Dothideomycete *Leptosphaeria maculans*. Mol. Microbiol. 60:67-80.

Hammond, K. E., and Lewis, B. G. 1987. The establishment of systemic infection in leaves of oilseed rape by *Leptosphaeria maculans*. Plant Pathol. 36:135-147.

Hammond-Kosack, K. E., and Jones, J. D. 1996. Resistance gene-dependent plant defense responses. Plant Cell 8:1773-1791.

Hanfrey, C., Fife, M., and Buchanan-Wollaston, V. 1996. Leaf senescence in *Brassica napus*: Expression of genes encoding pathogenesis-related proteins. Plant Mol. Biol. 30:597-609.

Hématy, K., Cherk, C., and Somerville, S. 2009. Host–pathogen warfare at the plant cell wall. Curr. Opin. Plant Biol. 12:406-413.

Iuchi, S., Kobayashi, M., Taji, T., Naramoto, M., Seki, M., Kato, T., Tabata, S., Kakubari, Y., Yamaguchi-Shinozaki, K., and Shinozaki, K. 2001. Regulation of drought tolerance by gene manipulation of 9-cis-epoxycarotenoid dioxygenase, a key enzyme in abscisic acid biosynthesis in *Arabidopsis*. Plant J. 27:325-333.

Jindrichova, B., Fodor, J., Sindelarova, M., Burketova, L., and Valentova, O. 2011. Role of hydrogen peroxide and antioxidant enzymes in the interaction between a hemibiotrophic fungal pathogen, *Leptosphaeria maculans*, and oilseed rape. Environ. Exp. Bot. 72:149-156.

Jones, J. D., and Dangl, J. L. 2006. The plant immune system. Nature 444:323-329.

Kaliff, M., Staal, J., Myrenas, M., and Dixelius, C. 2007. ABA is required for *Leptosphaeria maculans* resistance via ABI1- and ABI4-dependent signaling. Mol. Plant-Microbe Interact. 20:335-345.

Laudert, D., and Weiler, E. W. 1998. Allene oxide synthase: A major control point in *Arabidopsis thaliana* octadecanoid signalling. Plant J. 15:675-684.

Lee, J., Feng, J., Campbell, K. B., Scheffler, B. E., Garrett, W. M., Thibivilliers, S., Stacey, G., Naiman, D. Q., Tucker, M. L., Pastor-Corrales, M. A., and Cooper, B. 2009. Quantitative proteomic analysis of bean plants infected by a virulent and avirulent obligate rust fungus. Mol. Cell. Proteomics 8:19-31.

Li, J., Brader, G., and Palva, E. T. 2004. The WRKY70 transcription factor: A node of convergence for jasmonate-mediated and salicylate-mediated signals in plant defense. Plant Cell 16:319-331.

Liu, G., Kennedy, R., Greenshields, D. L., Peng, G., Forseille, L., Selvaraj, G., and Wei, Y. 2007. Detached and attached *Arabidopsis* leaf assays reveal distinctive defense responses against hemibiotrophic *Colletotrichum* spp. Mol. Plant-Microbe Interact. 20:1308-1319.

Marshall, O. J. 2004. PerlPrimer: Cross-platform, graphical primer design for standard, bisulphite and real-time PCR. Bioinformatics 20:2471-2472.

McDonald, B. A., and Linde, C. 2002. Pathogen population genetics, evolutionary potential, and durable resistance. Annu. Rev. Phytopathol. 40:349-379.

Mittler, R., and Lam, E. 1995. Identification, characterization, and purification of a tobacco endonuclease activity induced upon hypersensitive response cell death. Plant Cell 7:1951-1962.

Mur, L. A., Kenton, P., Lloyd, A. J., Ougham, H., and Prats, E. 2008. The hypersensitive response; the centenary is upon us but how much do we know? J. Exp. Bot. 59:501-520.

Norman-Setterblad, C., Vidal, S., and Palva, E. T. 2000. Interacting signal pathways control defense gene expression in *Arabidopsis* in response to cell wall-degrading enzymes from *Erwinia carotovora*. Mol. Plant-Microbe Interact. 13:430-438.

Oliver, R. P., and Ipcho, S.V. 2004. *Arabidopsis* pathology breathes new life into the necrotrophs-vs.-biotrophs classification of fungal pathogens. Mol. Plant Pathol. 5:347-352.

Oliver, R. P., and Solomon, P. S. 2010. New developments in pathogenicity and virulence of necrotrophs. Curr. Opin. Plant Biol. 13:415-419.

Parlange, F., Daverdin, G., Fudal, I., Kuhn, M. L., Balesdent, M. H., Blaise, F., Grezes-Besset, B., and Rouxel, T. 2009. *Leptosphaeria maculans* avirulence gene *AvrLm4-7* confers a dual recognition specificity by the *Rlm4* and *Rlm7* resistance genes of oilseed rape, and circumvents *Rlm4*-mediated recognition through a single amino acid change. Mol. Microbiol. 71:851-863.

Pellinen, R. I., Korhonen, M. S., Tauriainen, A. A., Palva, E. T., and Kangasjarvi, J. 2002. Hydrogen peroxide activates cell death and defense gene expression in birch. Plant Physiol. 130:549-560.

Perfect, S. E., and Green, J. R. 2001. Infection structures of biotrophic and hemibiotrophic fungal plant pathogens. Mol. Plant Pathol. 2:101-108.

Persson, M., Staal, J., Oide, S., and Dixelius, C. 2009. Layers of defense responses to *Leptosphaeria maculans* below the *RLM1*- and camalexin-dependent resistances. New Phytol. 182:470-482.

Pieterse, C. M., Leon-Reyes, A., Van der Ent, S., and Van Wees, S. C. 2009. Networking by small-molecule hormones in plant immunity. Nat. Chem. Biol. 5:308-316.

Potlakayala, S. D., Reed, D. W., Covello, P. S., and Fobert, P. R. 2007. Systemic acquired resistance in canola is linked with pathogenesis-related gene expression and requires salicylic acid. Phytopathology 97:794-802.

Rasmussen, U., Bojsen, K., and Collinge, D. B. 1992. Cloning and characterization of a pathogen-induced chitinase in *Brassica napus*. Plant Mol. Biol. 20:277-287.

Roussel, S., Nicole, M., Lopez, F., Renard, M., Chevre, A. M., and Brun, H. 1999. Cytological investigation of resistance to *Leptosphaeria maculans* conferred to *Brassica napus* by introgressions originating from *B. juncea* or *B. nigra* B genome. Phytopathology 89:1200-1213.

Rouxel, T., and Balesdent, M. H. 2005. The stem canker (blackleg) fungus, *Leptosphaeria maculans*, enters the genomic era. Mol. Plant Pathol. 6:225-241.

Rouxel, T., Grandaubert, J., Hane, J. K., Hoede, C., van de Wouw, A. P., Couloux, A., Dominguez, V., Anthouard, V., Bally, P., Bourras, S., Cozijnsen, A. J., Ciuffetti, L. M., Degrave, A., Dilmaghani, A., Duret, L., Fudal, I., Goodwin, S. B., Gout, L., Glaser, N., Linglin, J., Kema, G. H., Lapalu, N., Lawrence, C. B., May, K., Meyer, M., Ollivier, B., Poulain, J., Schoch, C.L., Simon, A., Spatafora, J.W., Stachowiak, A., Turgeon, B. G., Tyler, B. M., Vincent, D., Weissenbach, J., Amselem, J., Quesneville, H., Oliver, R. P., Wincker, P., Balesdent, M. H., and Howlett, B. J. 2011. Effector diversification within compartments of the *Leptosphaeria maculans* genome affected by repeat-induced point mutations. Nat. Commun. 2:202.

Schmidt, S. M., and Panstruga, R. 2011. Pathogenomics of fungal plant parasites: What have we learnt about pathogenesis? Curr. Opin. Plant Biol. 14:392-399.

Shibata, Y., Kawakita, K., and Takemoto, D. 2010. Age-related resistance of *Nicotiana benthamiana* against hemibiotrophic pathogen *Phytophthora infestans* requires both ethylene- and salicylic acid-mediated signaling pathways. Mol. Plant-Microbe Interact. 23:1130-1142.

Staal, J., Kaliff, M., Bohman, S., and Dixelius, C. 2006. Transgressive segregation reveals two *Arabidopsis* TIR-NB-LRR resistance genes effective against *Leptosphaeria maculans*, causal agent of blackleg disease. Plant J. 46:218-230.

Steiner, A. A. 1984. The universal nutrient solution. Pages 633-649 in: Proceedings of the Sixth International Congress on Soilless Culture, Wageningen, The Netherlands.

Tao, Y., Xie, Z., Chen, W., Glazebrook, J., Chang, H. S., Han, B., Zhu, T., Zou, G., and Katagiri, F. 2003. Quantitative nature of *Arabidopsis* responses during compatible and incompatible interactions with the bacterial pathogen *Pseudomonas syringae*. Plant Cell 15:317-330.

Torres, M. A., Jones, J. D., and Dangl, J. L. 2006. Reactive oxygen species signaling in response to pathogens. Plant Physiol. 141:373-378.

Tsuda, K., Sato, M., Stoddard, T., Glazebrook, J., and Katagiri, F. 2009. Network properties of robust immunity in plants. PLoS Genet. 5:e1000772.

Vlot, A. C., Dempsey, D. A., and Klessig, D. F. 2009. Salicylic acid, a multifaceted hormone to combat disease. Annu. Rev. Phytopathol. 47:177-206.

Wildermuth, M. C., Dewdney, J., Wu, G., and Ausubel, F. M. 2001. Isochorismate synthase is required to synthesize salicylic acid for plant defence. Nature 414:562-565.

Yu, I. C., Parker, J., and Bent, A. F. 1998. Gene-for-gene disease resistance without the hypersensitive response in *Arabidopsis dnd1* mutant. Proc. Natl. Acad. Sci. U.S.A. 95:7819-7824.